NJC

New Journal of Chemistry

An international journal of the chemical sciences

www.rsc.org/njc

Volume 32 | Number 8 | August 2008 | Pages 1269–1456



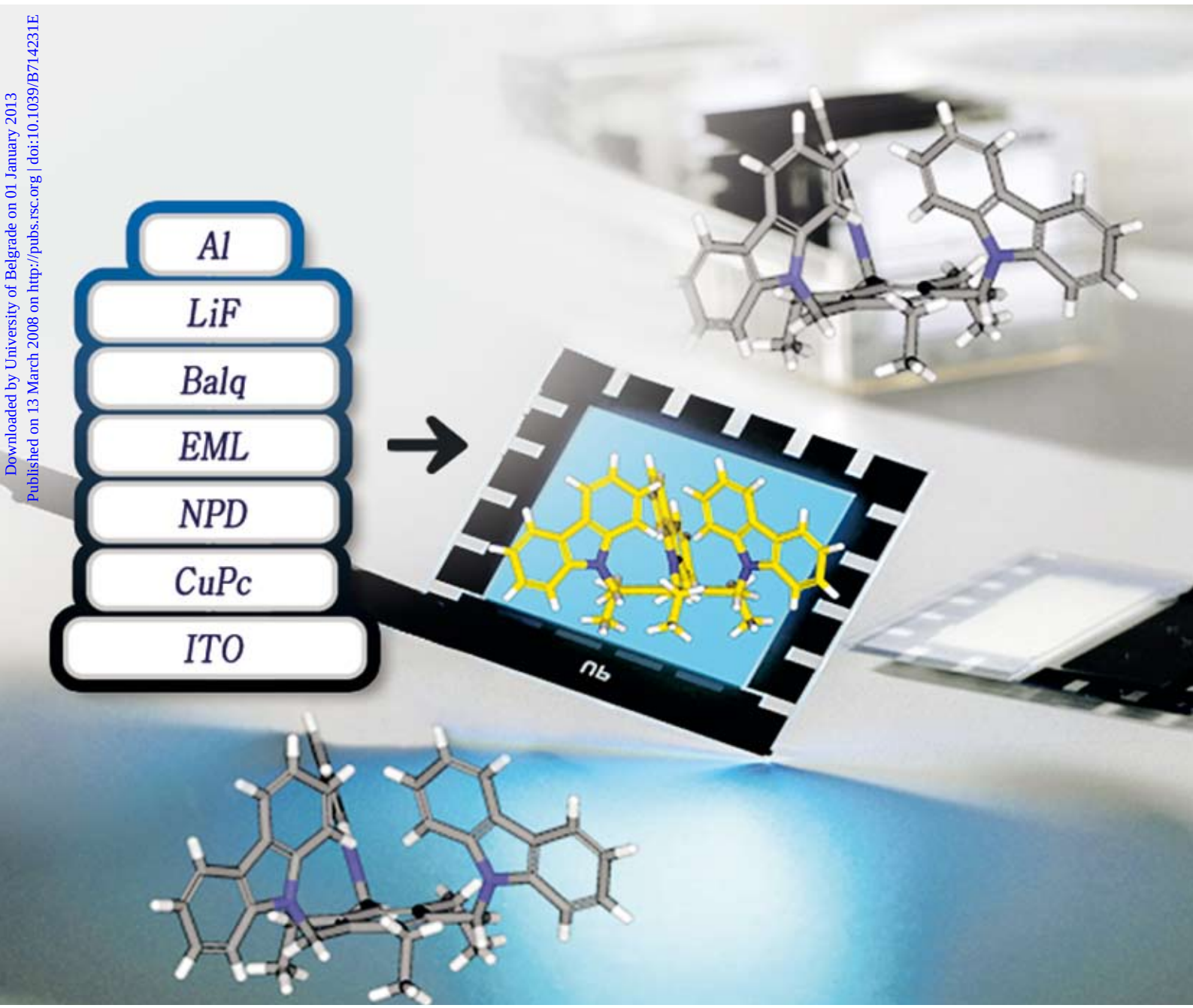


ISSN 1144-0546

RSC Publishing

CENTRE NATIONAL DE LA RECHERCHE SCIENTIFIQUE

**PAPER**

Jong-In Hong *et al.*

Efficient blue phosphorescent host through nonbonded conformational locking interactions

# Efficient blue phosphorescent host through nonbonded conformational locking interactions†

**Jongchul Kwon,[a] Tae-Hyuk Kwon,[a] Hyo Soon Cho,[a] Myoung Ki Kim,[a] Ik-Soo Shin,[a] Dae-Yup Shin,[b] Su Jin Park[b] and Jong-In Hong*[a]**

***Received (in Durham, UK) 14th September 2007, Accepted 6th February 2008***
***First published as an Advance Article on the web 13th March 2008***
**DOI: 10.1039/b714231e**



We developed a new host material TCTEB with a conformationally homogeneous, sterically bulky structure due to nonbonded interactions between adjacent methylene groups. The host presented good thermal stability ($T_g$ = 122 °C and $T_d$ = 321 °C) and high triplet energy (3.0 eV). The maximum quantum efficiency, current efficiency and power efficiency of the OLED device using the TCTEB host were 8.5%, 13.7 cd $A^{-1}$, and 11.3 lm $W^{-1}$, respectively, when doped with 8 wt% FIrpic.

## Introduction

Since the first introduction of organic light-emitting diodes (OLEDs) by Tang and VanSlyke,[1] the development of OLEDs has received considerable attention because of their possible application to full color displays. It is well known that the selection of an appropriate combination of dopant and host materials in the emitting layer is a prerequisite for the development of an efficient OLED device, although the resulting efficiency of the device is controlled by the total capability of each layer in the device. Phosphorescent dopant materials have been more attractive in comparison with fluorescent materials because they can reach an internal quantum efficiency of 100% through the radiative recombination of both singlet and triplet excitons.[2] Although highly efficient and long-lived red and green phosphorescent materials have been developed,[3] stable blue materials with high efficiency have not yet been realized because it is still very difficult to obtain a host with triplet energy [4–8,12] high enough to transfer its energy to the blue dopant, as well as good charge transport ability.[8]

Carbazole derivatives have been utilized in the construction of highly photoconductive amorphous organic materials and thus they have been used in OLED materials as hole transport material *via* radical cation species[14,15] or as host material.[4,5,16] Due to its high triplet energy (*ca.* 3.0 eV), carbazole can be a good candidate for a blue phosphorescent host material if its low thermal stability can be improved and if its flat structure, which tends to promote crystallization,[16] can be avoided through conformational control.

To overcome the above issues, we designed carbazole based new host materials that have three carbazole groups at the 1,3,5-benzylic positions of hexaethylbenzene while maintaining the triplet energy of carbazoles with a reasonable $T_g$ value. Here we report the synthesis of TCTEB, and the OLED device study using TCTEB as a novel host that can reduce luminance quenching *via* self-aggregation among the flat carbazole structures through nonbonded, conformational locking interactions in TCTEB. TCTMB was also used as another host for comparison with the device using TCTEB. The concept behind the design of TCTEB derives from the conformation of hexaethylbenzene. The lowest energy conformation of hexaethylbenzene has the ethyl groups oriented perpendicular to the central ring in a fully alternated up–down disposition.[9–11] In this arrangement, the three ethyl groups at the 1, 3, and 5 positions of the central ring are all pointing towards the same face of the aryl ring, while the rest of the ethyls point in the opposite direction. Molecular mechanics calculations predict that the fully alternated conformation of hexaethylbenzene is *ca.* 3.5 kcal $mol^{-1}$ lower in energy than a non-alternated conformation possessing two pairs of adjacent ethyl groups with a syn arrangement.[9–11] This results from the avoidance of nonbonded interactions of the adjacent methylene hydrogens (Fig. 1, left). It has also been reported that hexasubstituted benzene derivatives, possessing substituents nearly isosteric with ethyl groups, adopt a similar conformation. Thus, TCTEB would adopt a conformation with full up–down alternation of the side arms in which the three carbazolyl groups are pointing toward the same face of the central benzene ring. This was supported by the energy-minimized structure of TCTEB (Fig. 1). However, in the case of TCTMB, carbazolyl methyl groups are more randomly oriented, compared to those of TCTEB, because the carbazolyl methyl groups are expected to point either up or down around the benzene ring while maintaining the $C_{ar}C_{ar}CH_2N$ dihedral angles near 90°. The only difference between TCTEB and TCTMB is that TCTEB is conformationally more rigid than TCTMB. The three carbazolyl groups of TCTEB are converged and therefore are less likely to be self-aggregated compared to TCTMB. In the case of TCTMB, the three carbazolyl groups are either pointing in the same direction or one of them is pointing away from other the two carbazolyl groups and thus more likely to be self-aggregated compared to TCTEB.

[a] *Department of Chemistry, College of Natural Sciences, Seoul National University, Seoul 151-747, Korea. E-mail: jihong@snu.ac.kr; Fax: +82-2-889-1568; Tel: +82-02-880-6682*
[b] *Corporate R&D Center, Samsung SDI, Yongin 449-902, Korea*
† Electronic supplementary information (ESI) available: CV, TGA, DSC, more detailed device data, and DFT calculations. See DOI: 10.1039/b714231e

 

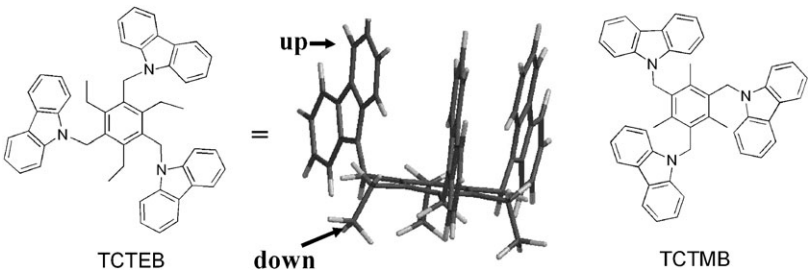


**Fig. 1** Molecular structures of TCTEB (left) and TCTMB (right), and the energy minimized structure of TCTEB (middle).



## Experimental section

### Synthesis

$^1$H and $^{13}$C NMR spectra were recorded using an Advance 300 MHz Bruker spectrometer in $CDCl_3$. $^1$H NMR chemical shifts in $CDCl_3$ were referenced to $CHCl_3$ (7.27 ppm), and $^{13}$C NMR chemical shifts in $CDCl_3$ were reported relative to $CHCl_3$ (77.23 ppm). UV visible spectra were recorded on a Beckman DU650 spectrophotometer. Fluorescence spectra were recorded on a Jasco FP-7500 spectrophotometer. Mass spectra were obtained using a MALDI-TOF MS from Bruker. High resolution masses were measured by FAB mass using JEOL HP 5890 series. Analytical thin-layer chromatography was performed using Kieselgel 60F-254 plates from Merck. Column chromatography was carried out on Merck silica gel 60 (70–230 mesh). All solvents and reagents were commercially available and used without further purification unless otherwise noted. Decomposition temperatures were obtained using a Thermo Gravimetric Analyzer (TGA) from Rheometric Scientific. Glass transitions temperatures were recorded on a Jasco FP-750 spectrophotometer Differential Scanning Calorimetry (DSC) from TA Instruments. 1,3,5-Tris(bromomethyl)-2,4,6-triethylbenzene (**1**) and 1,3,5-tris(bromomethyl)-2,4,6-trimethylbenzene (**2**) were synthesized according to a literature procedure.[11]

**TCTEB (1,3,5-*N*,*N*′,*N*″-tricarbazolylmethyl-2,4,6-triethylbenzene).** A mixture of 1,3,5-tris(bromomethyl)-2,4,6-triethylbenzene (1.02 g, 2.31 mmol), carbazole (1.55 g, 9.24 mmol), and $Cs_2CO_3$ (3.76 g, 11.5 mmol) in *N*,*N*′-dimethylformamide (DMF) was heated at 70 °C under continuous stirring for 12 h. After cooling to room temperature, the solvent was evaporated in high vacuum and reaction mixture was extracted with methylene chloride. The organic phase was washed with water and dried over $Na_2SO_4$. The solvent was evaporated to give the crude product, which was applied to column chromatography on silica gel using methylene chloride, hexane as eluent and recrystallized from methylene chloride and hexane to give a white solid product (Yield: 591 mg, 37%). $^1$H NMR (300 MHz, $CDCl_3$): $\delta$ (ppm) 8.08 (d, 6 Hz, 6H), 7.21 (d, 9 Hz, 6H), 7.18 (d, 12 Hz, 6H), 7.13 (d, 12 Hz, 6H), 5.58 (s, 6H), 2.91 (q, 21 Hz, 6H), 0.94 (t, 15 Hz, 9H). $^{13}$C NMR (125 MHz, $CDCl_3$): $\delta$ (ppm) 146.0, 140.9, 141.9, 126.1, 123.5, 120.4, 119.2, 109.8, 43.3, 23.9, 15.2. HRMS (FAB): calcd. for $C_{51}H_{45}N_3$ 699.3613 g mol$^{-1}$, found 699.3613 g mol$^{-1}$.

**TCTMB (1,3,5-*N*,*N*′,*N*″-tricarbazolylmethyl-2,4,6-trimethylbenzene).** A mixture of 1,3,5-tris(bromomethyl)-2,4,6-trimethylbenzene (2.00 g, 5.01 mmol), carbazole (3.41 g, 20.4 mmol), and $Cs_2CO_3$ (8.18 g, 25.1 mmol) in DMF was heated to 70 °C under continuous stirring for 12 h. The reaction mixture was cooled to room temperature and solvent was evaporated and the residue was dissolved in methylene chloride. The crude product was recrystallized from $CH_2Cl_2$–hexane to give a white solid (Yield: 1.25 g, 38%). $^1$H NMR (300 MHz, $CDCl_3$): $\delta$ (ppm) 8.08 (d, 9 Hz, 6H), 7.24 (t, 6 Hz, 6H), 7.20 (d, 6 Hz, 6H), 7.10 (d, 9 Hz, 6H), 5.56 (s, 6H), 2.29 (s, 9H). $^{13}$C NMR (75 MHz, $CDCl_3$): $\delta$ (ppm) 140.6, 138.6, 134.5, 132.4, 125.9, 123.2, 120.3, 119.0, 109.4, 44.2, 17.4. MALDI-TOF: calcd. for $C_{48}H_{39}N_3$ 657.31 g mol$^{-1}$, found 657.47 g mol$^{-1}$.

## Results and discussion

1,3,5-Tris(bromomethyl)-2,4,6-triethylbenzene (**1**) and 1,3,5-tris(bromomethyl)-2,4,6-trimethylbenzene (**2**) were synthesized according to a literature procedure.[11] TCTEB and TCTMB were synthesized by coupling carbazoles with 1,3,5-tris(bromomethyl)-2,4,6-triethylbenzene and 1,3,5-tris(bromomethyl)mesitylene, respectively (Scheme 1).

The absorption spectra of TCTEB and TCTMB (0.02 mM in $CH_2Cl_2$) are similar to that of carbazole except for the larger extinction coefficient due to the presence of three carbazole units in TCTEB and TCTMB (Fig. 2 and Table 1). The phosphorescence of each host was obtained in a frozen 2-methyltetrahydrofuran solution at 77 K. The fluorescence emission maximum wavelengths of TCTMB and TCTEB appear at 350 and 351 nm, respectively, and the phosphorescence triplet emission of TCTMB and TCTEB appears at the same wavelength ($\lambda$ = 413 nm), which was determined by taking the first emission peak of phosphorescence as the transition energy of $T_1 \rightarrow S_0$,[12] (Fig. 2a and b). The triplet emission (triplet energy 3.00 eV, the arrow in Fig. 2) of both TCTMB and TCTEB is blue-shifted compared to that of

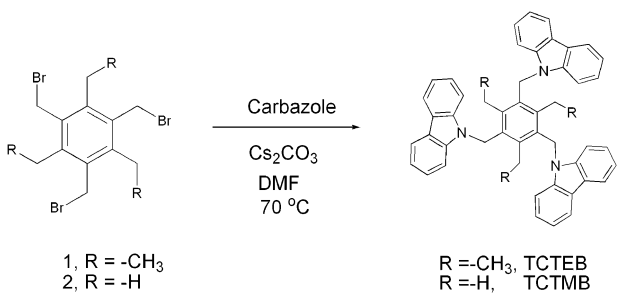


**Scheme 1** Synthesis of TCTEB and TCTMB.

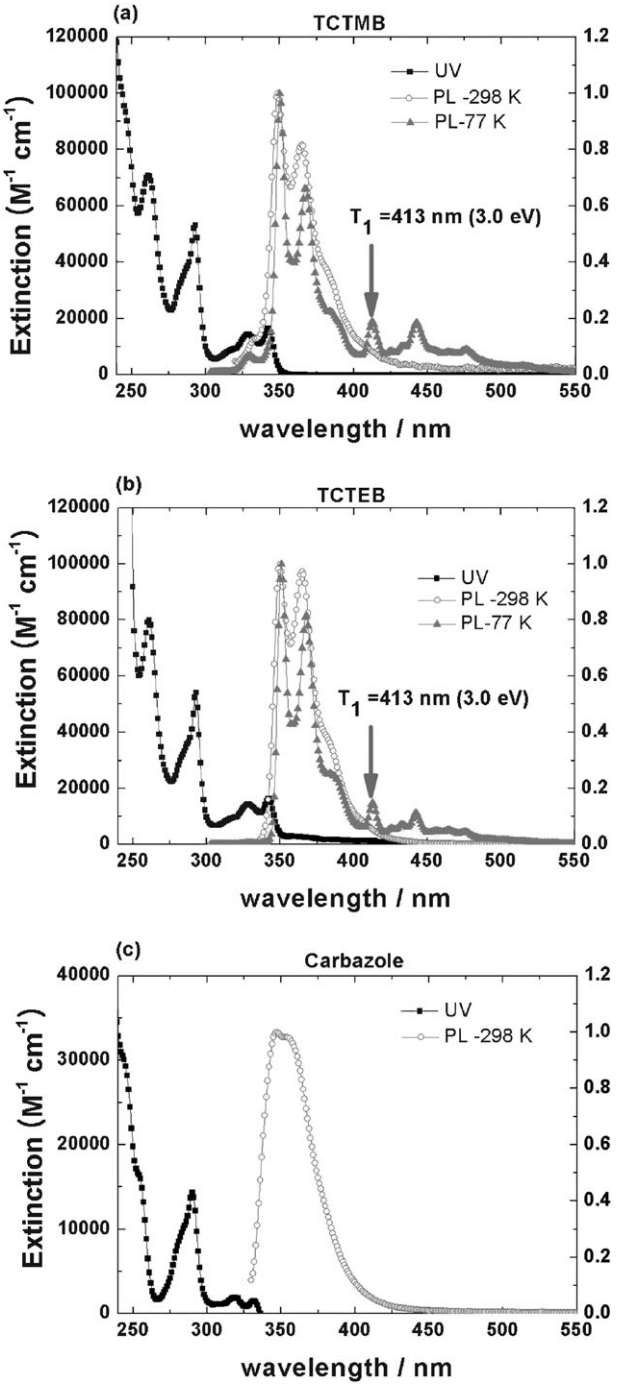


**Fig. 2** UV (0.02 mM in $CH_2Cl_2$) and PL spectra (0.02 mM in 2-methyltetrahydrofuran (2-MeTHF)) at 298 K and 77 K (a) TCTMB (b) TCTEB (c) carbazole.

*N*,*N*′-dicarbazolyl-4,4′-biphenyl (CBP, triplet energy 2.56 eV).[4] This is in good correlation with DFT calculations (see ESI†) Since the triplet energy of iridium(III) bis[(4,6-difluorophenyl)pyridinato-*N*,$C^{2'}$]picolinate (FIrpic) is 2.65 eV, the reverse energy transfer from the guest to the host can be prevented (Fig. 3a, Inset).

HOMO energy value of TCTEB was estimated from the cyclic voltammetry (CV). This electrochemical experiment was referenced with respect to a silver wire as the quasi-reference electrode (AgQRE) at room temperature and then calibrated to a standard hydrogen electrode (SHE) using ferrocene ($Fc/Fc^+$). Acetonitrile solutions for cyclic voltammetry contained a 2 mm diameter Pt working electrode, a Pt counter electrode, and a 0.1 M $TBAPF_6$ (tetra-*n*-butylammonium hexafluorophosphate) supporting electrolyte. The oxidation potential of TCTEB is observed at $E_{1/2}$ = 1.50 V *vs*. SHE. The HOMO energy level of TCTEB (−5.99 eV) is calculated from $E_{1/2}$ after correction of the vacuum energy level (4.49 eV)[13] which is similar to that of FIrpic (−5.8 eV)[12] (Table 1).

Such a sterically bulky and conformationally homogeneous molecular structure of TCTEB is beneficial to the thermal stability and morphological stability. This is indicated by the high glass-transition temperature ($T_g$) of 122 °C, measured by DSC (differential scanning calorimetry), and a high decomposition temperature ($T_d$) of 321 °C—which corresponds to a 5% weight loss in thermogravimetric analysis (TGA)—under a $N_2$ stream with a scanning rate of 10 °C $min^{-1}$. TCTEB has a higher $T_g$ value compared to the known carbazole based blue host material, *N*,*N*′-dicarbazolyl-3,5-benzene (mCP, $T_g$ < 60 °C),[12] and it is difficult to crystallize and can form a homogeneous and stable film after vacuum deposition.[12] TCTMB also exhibited a high $T_d$ value of 377 °C.

Organic layers were fabricated by high-vacuum ($10^{-7}$ torr) thermal evaporation onto a patterned ITO glass pre-cleaned by a UV-ozone chamber. The 10 nm-thick film of copper phthalocyanine (CuPc) and 30 nm-thick film of 4,4′-bis[*N*-(naphthyl-*N*-phenylamino)biphenyl (α-NPD) served as a hole injection layer (HIL) and a hole transport layer, respectively. The EML was prepared by co-evaporating a TCTEB or TCTMB host and *x* wt% FIrpic dopant. Dopant concentration is in the 6–11 wt% range. Next, a 30 nm-thick 4-biphenyloxolatoaluminium(III)bis(2-methyl-8-quinolinato)4-phenylphenolate (BAlq) layer, as both a hole blocking layer (HBL) and electron transporting layer (ETL), was deposited, which was then followed by deposition of LiF as an electron injection layer. Finally, after changing the metal mask, a 100 nm thick aluminium film was deposited on the EIL and then encapsulated so as not to be exposed to oxygen and moisture. The Keithly 2400 as a source meter with a computer was used to operate the device.

Fig. 3 compares the current density *versus* voltage (a) and external quantum efficiencies as a function of current density (b) obtained for both TCTMB (8 wt% FIrpic) and TCTEB (6–11 wt% FIrpic) devices, and all device results are summarized in Table 2. Although the energy levels of TCTMB and TCTEB are similar, the current density of TCTMB is significantly lower than that of TCTEB. The turn-on voltage of TCTEB at 1 cd $m^{-2}$ is in the range of 4.2–4.8 V depending on the doping ratio while that of TCTMB significantly increases up to 9.6 V as shown in Table 2. We assume that the low current density and high turn-on voltage of TCTMB are presumably due to rather facile self-aggregation of TCTMB. TCTMB exhibits very poor solubility in any organic solvent and is easily precipitated while TCTEB is more easily soluble in $CH_2Cl_2$ solution due to the ethyl groups. Thus, deposited on the emitting layer, TCTMB could be easily crystallized and thus might decrease the carrier mobility in the device. Using 8 wt% FIrpic in TCTEB, we obtain a peak external quantum

 

**Table 1** Photophysical and electrochemical data for TCTMB, TCTEB and carbazole

| Compound | Abs $\lambda$ ($\varepsilon \times 10^5$ $M^{-1}$ $cm^{-1}$)[a] | Emission ($\lambda_{max}$ nm)[b] 298 K | 77 K[e] | HOMO[c] | $\Delta E$[d] $S_1(T_1)$ |
|---|---|---|---|---|---|
| TCTMB | 238 (1.2), 261 (0.71), 293 (0.53), 329 (0.14), 342 (0.16) | 349 | 413 | | 3.55 (3.00) |
| TCTEB | 248 (>2), 261 (0.80), 293 (0.54), 328 (0.14), 342 (0.16) | 349 | 413 | 5.99 | 3.55 (3.00) |
| Carbazole | 227 (1.25), 234 (0.46), 253 (0.17), 290 (0.14), 319 (0.02), 332 (0.02) | 347 | | | |

[a] The absorption spectra were measured in 0.02 mM $CH_2Cl_2$ solution. [b] The emission spectra were measured in 0.02 mM 2-MeTHF solution. [c] All potentials were determined at room temperature in acetonitrile solutions (0.1 M $TBAPF_6$) *vs.* AgQRE. $E_{HOMO} = E_{1/2}^{ox} + 4.49$ eV. [d] $\Delta E$ = HOMO–LUMO. Singlet energy gap was calculated from the cross section wavelength between absorption and emission spectra. Triplet energy gap was measured from the first peak wavelength at low temperature PL. [e] The first singlet peak in the low temperature PL at 77 K.

efficiency of 8.5% at 1.8 J (mA $cm^{-2}$) which corresponds to efficiencies of 13.8 cd $A^{-1}$ and 11.4 lm $W^{-1}$. The electroluminescence (EL) spectrum is seen to be entirely due to FIrpic emission with Commission Internationale de l'Eclairage (CIE) coordinates of (0.17, 0.36) at 1 mA $cm^{-2}$.

Table 2 shows that the performance of the device derived from FIrpic and TCTEB is superior to the performance of the device derived from CBP and FIrpic ($\eta_{ext}$ = 6.1%, $\eta_p$ = 7.8 lm $W^{-1}$).[17]† This is because the FIrpic and CBP device system shows endothermic energy transfer between the dopant and the host and therefore the reverse energy transfer from the dopant to the host cannot be prevented. Furthermore, compared with the device derived from mCP having similar triplet energy,[6] the performance measured with the TCTEB device system exhibited better results. Especially, the maximum luminous power efficiency of the TCTEB device system (Max $\eta_p$ = 11.3 lm $W^{-1}$) is higher than that of the mCP and FIrpic device system (Max $\eta_p$ = 8.9 lm $W^{-1}$),[6] while the maximum quantum efficiency (Max $\eta_{ext}$ = 8.5%) is slightly higher than that of the mCP device system (Max $\eta_{ext}$ = 7.5%). One reason for this result may be related to charge carrier injection or carrier mobility. It has been previously reported that the mCP derived device system exhibited a slightly larger turn-on voltage compared to the CBP device system and similar charge injection or mobility.[6] This result suggests that higher efficiency of the mCP device system, compared to the CBP device system, does not result from the improved carrier injection or carrier mobility but from the higher quantum efficiency and exothermic energy transfer between FIrpic and mCP. In the case of the TCTEB device (see Fig. S4 and Table 2), not only the charge injection but also the turn-on voltage are slightly better than those of the CBP device. Thus, the reason for higher power luminous efficiency of the TCTEB device compared to the mCP device, although they have similar triplet energies, would be the improved charge injection or carrier mobility. Another reason for the improved device

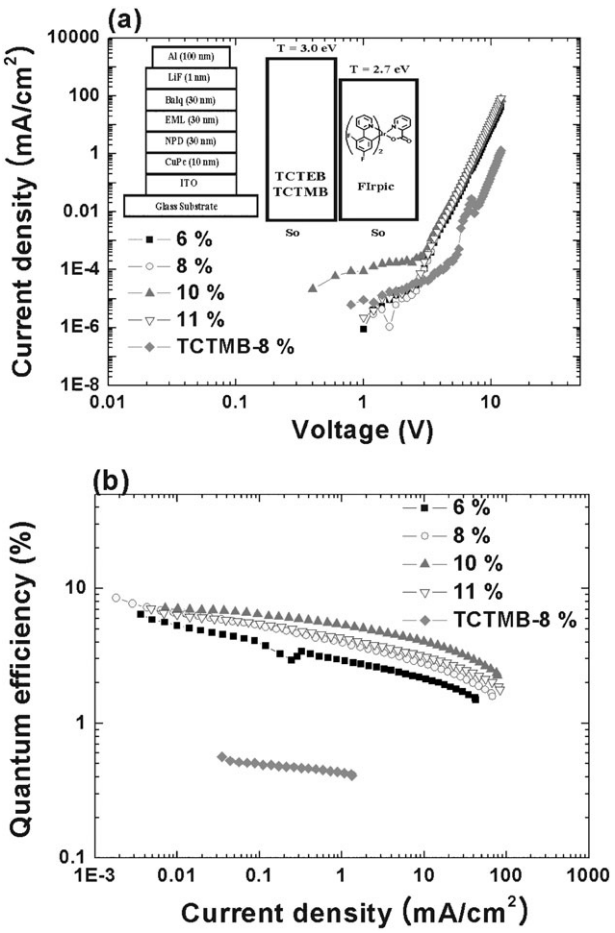


**Fig. 3** EL device data when TCTEB or TCTMB is doped with *x* wt% FIrpic (*x* = 6–11). (a) Voltage *vs.* Current density J (mA $cm^{-2}$). Inset shows the device configuration and triplet energy level of TCTEB or TCTMB and FIrpic, respectively, obtained from a frozen 2-methyltetrahydrofuran solution at 77 K. (b) Current density J (mA $cm^{-2}$) *vs.* quantum efficiency.

**Table 2** OLED performance of devices derived from TCTEB and TCTMB hosts

| Host (wt%)[a] | Max $\eta_{ext}$ (%) | Max $\eta_p$ (lm $W^{-1}$) | Max $\eta_c$ (cd $A^{-1}$) | $V_{turn\ on}$[b] |
|---|---|---|---|---|
| CBP | 6.1 | 7.8 | 10.4 | 4.6 |
| (6 %) | (3.0)[c] | (1.9) | (5.8) | |
| TCTEB | 6.4 | 8.4 | 11.2 | 4.8 |
| (6 %) | (2.1)[c] | (1.3) | (4.3) | |
| TCTEB | 8.5 | 11.3 | 13.7 | 4.6 |
| (8 %) | (2.7) | (1.7) | (5.6) | |
| TCTEB | 7.2 | 10.3 | 13.8 | 4.2 |
| (10 %) | (4.0) | (2.7) | (8.2) | |
| TCTEB | 7.1 | 9.5 | 12.8 | 4.4 |
| (11 %) | (3.8) | (2.8) | (7.7) | |
| TCTMB | 0.56 | 0.33 | 0.92 | 9.6 |
| (8 %) | | | | |

[a] FIrpic doping ratio. ITO/CuPC (10 nm)/NPD (30 nm)/EML (30 nm) FIrpic *x* wt% doping /BAlq (30 nm)/LiF (1 nm)/Al (100 nm). [b] Turn-on voltage was estimated from the point of 1 cd $m^{-2}$. [c] All data in parentheses were obtained at 10 mA $cm^{-2}$.

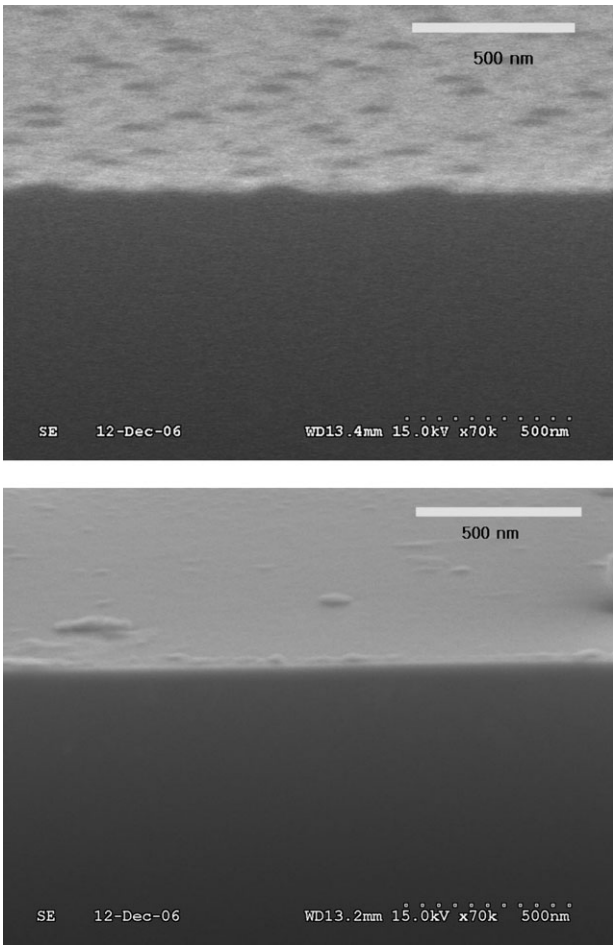


**Fig. 4** FE-SEM images of TCTMB (top) and TCTEB (bottom) doped with 8 wt% FIrpic on a silicon wafer.

performance of the TCTEB device system would be a sterically bulky structure of TCTEB, preventing self-quenching which is detrimental to the device performance in the emitting layer.

The poor performance is most likely due to the low carrier mobility resulting from crystallization or self-aggregation of TCTMB. This hypothesis was supported by the FE-SEM images of TCTMB and TCTEB, both doped with 8 wt% FIrpic on a silicon wafer (Fig. 4). After deposition on a silicon wafer, TCTMB displays poor morphology presumably due to self-aggregation or crystallization while TCTEB exhibits good morphology due to the reduced conformational space through the nonbonded interactions. Ethyl groups in TCTEB are likely to lead to a conformationally homogenous and sterically bulky host structure, which eventually might result in higher carrier mobility in the resulting device compared to the device derived from the TCTMB host. As the doping ratio of FIrpic increases from 6 wt% to 11 wt%, in the case of the TCTEB host, the device performance at high current density gradually increases up to a ratio of 10 wt% although the maximum efficiency at 10 wt% of the doping ratio is a little lower than that at 8 wt%. At 10 mA $cm^{-2}$, the external quantum efficiency, current efficiency and power efficiency of 10 wt% FIrpic doped into the TCTEB host are 4.0%, 8.2 cd $A^{-1}$, and 4.0 lm $W^{-1}$, respectively. In the case of 11 wt% FIrpic, the device still exhibits a higher performance (3.8%, 7.7 cd $A^{-1}$, and 2.8 lm $W^{-1}$) than in the case of 8 wt% FIrpic (2.7%, 5.6 cd $A^{-1}$, and 1.7 lm $W^{-1}$) at 10 mA $cm^{-2}$.

## Conclusions

In conclusion, we have developed a new host material TCTEB with a conformationally homogenous, sterically bulky structure due to nonbonded interactions between adjacent methylene groups. The host presented good thermal stability ($T_g$ = 122 °C and $T_d$ = 321 °C) and high triplet energy (3.0 eV). The maximum quantum efficiency, current efficiency and power efficiency of the OLED device using the TCTEB host showed 8.5%, 13.7 cd $A^{-1}$, and 11.3 lm $W^{-1}$, respectively, when doped with 8 wt% FIrpic. This is remarkable in that TCTEB shows much better device data compared to the structurally similar TCTMB.

## Acknowledgements

We thank the Samsung SDI-SNU grant and the Seoul R&BD Program for the financial support. We also acknowledge the BK 21 fellowship grants to T.-H.K and J.K.

## References

1. C. W. Tang and S. A. VanSlyke, *Appl. Phys. Lett.*, 1987, **51**, 913.
2. C. Adachi, M. A. Baldo, S. R. Forrest and M. E. Thompson, *Appl. Phys. Lett.*, 2000, **77**, 904.
3. R. C. Kwong, M. S. Weaver, M.-H. M. Lu, Y.-J. Tung, A. B. Chwang, T. X. Zhou, M. Hack and J. J. Brown, *Org. Electron.*, 2003, **4**, 155.
4. R. J. Holmes, S. R. Forrest, Y.-J. Tung, R. C. Kwong, J. J. Brown, S. Garon and M. E. Thompson, *Appl. Phys. Lett.*, 2003, **82**, 2422.
5. S. Tokito, T. lijima, Y. Suzuri, H. Kita, T. Tsuzuki and F. Sato, *Appl. Phys. Lett.*, 2003, **83**, 569.
6. R. J. Holmes, B. W. D'Andrade, S. R. Forrest, X. Ren, J. Li and M. E. Thompson, *Appl. Phys. Lett.*, 2003, **83**, 3818.
7. P. E. Burrows, A. B. Padmaperuma, L. S. Sapochak, P. Djurovich and M. E. Thomson, *Appl. Phys. Lett.*, 2006, **88**, 183503.
8. P. A. Vecchi, A. B. Padmaperuma, H. Qiao, L. S. Sapochak and P. E. Burrows, *Org. Lett.*, 2006, **8**, 4211.
9. D. J. Iverson, G. Hunter, J. F. Blount, J. R. Damewood, Jr and K. Mislow, *J. Am. Chem. Soc.*, 1981, **103**, 6073.
10. H. E. Gottlieb, C. Ben-Ari, A. Hassner and V. Marks, *Tetrahedron*, 1999, **55**, 4003.
11. A. Vacca, C. Nativi, M. Cacciarini, R. Pergoli and S. Roelens, *J. Am. Chem. Soc.*, 2004, **126**, 16456.
12. M.-H. Tsai, H.-W. Lin, H.-C. Su, T.-H. Ke, C.-c. Wu, F.-C. Fang, Y.-Li. Liao, K.-T. Wong and C.-I. Wu, *Adv. Mater.*, 2006, **18**, 1216.
13. J. Lu, Y. Tao, M. D'iorio, Y. Li, J. Ding and M. Day, *Macromolecules*, 2004, **37**, 2442.
14. B. Gómez-Lor, B. Alonso, A. Omenat and J. L. Serrano, *Chem. Commun.*, 2006, 5012.
15. B. E. Koene, D. E. Loy and M. E. Thompson, *Chem. Mater.*, 1998, **10**, 2235.
16. V. Adamovich, J. Brooks, A. Tamayo, A. M. Alexander, P. I. Djurovich, B. W. D'Andrade, C. Adachi, S. R. Forrest and M. E. Thompson, *New J. Chem.*, 2002, **26**, 1171.
17. C. Adachi, R. C. Kwong, P. Djurovich, V. Adamovich, M. A. Baldo, M. E. Thompson and S. R. Forrest, *Appl. Phys. Lett.*, 2001, **79**, 2082.

 